X-RAY COMPUTED TOMOGRAPHY CHARACTERISING CARBON FIBER REINFORCED COMPOSITES

E. Cornelis[1]
A. Kottar, H. P. Degischer[2]

[1] Dept. of Physics – Visionlab, Univ. of Antwerp, Groenenborgerlaan 171, B2020 Antwerpen, Belgium
[2] Inst. of Materials Science and Testing, Vienna Univ. of Technology, Karlsplatz 13, A-1040 Wien Austria.

ABSTRACT

Continuous C-fibers are used to reinforce polymers (CFRP) and light metals (CFRM). Preforms are made of tows consisting of thousands of unidirectional fibers. Layers of different fiber orientations or layers of woven fabrics are embedded in the selected matrix. High resolution X-ray micro-tomography (μXCT) reveals non-destructively the arrangement of the fiber bundles in aluminum, magnesium and epoxy matrix as well as inhomogeneities within the matrix. The low absorption of X-rays of these light materials allows to apply X-rays excited between 50 and 80 kV to provide reasonable material contrast.
The course of the fiber bundles can be observed by scanning through the reconstructed 3D images. Fiber free matrix regions can be depicted by iso-surfaces of the interface towards reinforced sections and their extension can be measured. The gray-value histograms of whole samples and segments thereof can be determined quantitatively. Benchmark histograms of composites with densely packed fiber arrangements in dense matrix can be specified. A quantitative quality criterion for uniformity of fiber packing and homogeneity of the matrix can be defined by the percentage of agreement between XCT gray-value histograms and the benchmark curve of a perfect composite.

KEYWORDS : non destructive testing, carbon fiber composite, fiber distribution, computed X-ray tomography, continuous fiber reinforced magnesium, aluminum, polymer

1. INTRODUCTION

C-fiber reinforcement of light materials is considered, when high specific strength and stiffness are required. Fiber tows are wound or fabrics are stapled to prepare preforms, which are infiltrated by polymers (CFRP) or metals in liquid state (CFRM), both of which are described by a recent overview on composite materials [1] [2] . The properties of continuous C-fiber reinforced composites are sensitive to the fiber orientation owing to the reinforcing mechanisms, but in addition due to the high anisotropy of C-fibers. Unidirectional (UD) C-fiber reinforcement of metals yields improvements in fiber direction, but degrades the matrix properties in transverse direction [3]. Non-destructive determination of fiber orientation and their three-dimensional (3D) arrangement in the composite provides the structural information for the prediction of CFRM and CFRP properties. X-ray tomography (XCT) became an efficient research tool for investigation of heterogeneous materials [4], which is applied to determine non-destructively the C-fiber arrangement in Mg and Al, as well as in epoxy matrix. Furthermore inhomogeneities in the matrix, like porosities or cracks can be detected. The exploitation of XCT by high resolution techniques (μXCT) for quantitative measures of the quality of continuous carbon fiber reinforced light materials as far as fiber arrangement and matrix homogeneity are concerned, will be shown by means of a few examples.

2. EXPERIMENTAL DETAILS

2.1 Continuous fiber reinforced light metals (CFRM)

The investigated Mg and Al matrix composites reinforced with continuous C-fibers have been produced by gas pressure infiltration by Leichtmetall-Kompetenzzentrum Ranshofen/Austria

(LKR) [5] and Institut für Leichtbau und Kunststofftechnik, TU-Dresden/Germany (ILK) [6] as indicated in Table 1. Tows of high modulus (M40) fibers were wound to obtain densely packed UD fiber preforms for 2 mm thick plates. UD fabrics have been stapled alternatively in 0/±60° orientations, whereas 0/90° woven fabrics of high strength (T300) fibers parallel to each other. These preforms have been compressed to produce plate-like samples and additional pressure acted on the fiber bundles by the infiltration front of the non-wetting melt.

Table 1: *Specification of investigated metal matrix composites (CFRM)*

Acronym	Matrix	C-Fibers	Arrangement	v_f [%]	Source	Dimensions
Al/M40/UD	Al(99.85)	M40B	unidirectional wound	74±3	LKR	Plates 150×65×2 mm³
Mg/M40/UD	MgAl0.6	M40	unidirectional wound	70±1	LKR	
Al/M40/st0/±60°	Al(99.85)	M40B	[0,60,2(-60),60,0°]staple	64±4	LKR	
Mg/T300/w0/90°	MgAl0.2	T300J	0/90° weaves(50%/50%)	55±3	ILK	Rods 15×5×2mm³

The fiber distribution is observed on polished samples prepared by traditional preparation procedures for both optical and scanning electron microscopy. The fibers are densely packed in the UD samples yielding up to 77 vol.% locally, where the original fiber tows can hardly be recognized (Fig. 1), but there are matrix veins between fiber bundles. Micrographs in Fig. 2 show a CFRM samples with 6 UD fiber layers stapled symmetrically in orientations differing by 60° or 120°. There are fiber free matrix layers in between the differently oriented fiber layers, but not between the centrally placed parallel ones. Fig. 3 gives cross sectional and in-plane views of Mg/T300/w0/90° (50% in each direction), where the fibers are densely packed within the fiber bundles of the woven fabrics, but the bundles are clearly separated [7].

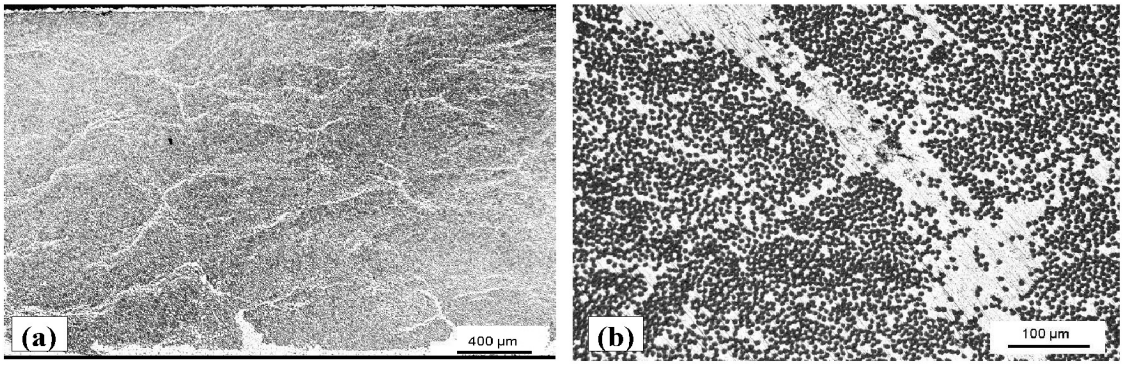

Fig. 1 Optical micrographs of cross sections of unidirectional C-fiber reinforced composites showing matrix veins between some fiber bundles: (a) Al/M40/UD; (b) Mg/M40/UD

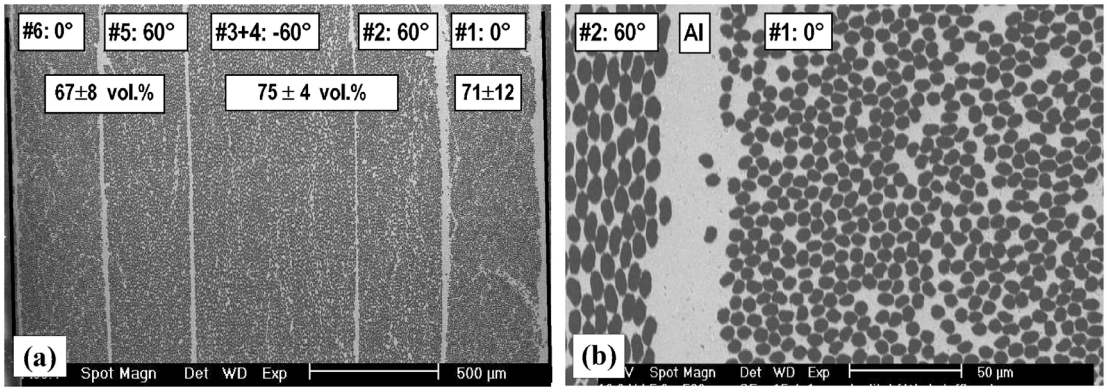

Fig. 2 SEM pictures of Al/M40/st0,±60° showing (a) the cross section of the 6 layers with their fiber orientation and volume fraction; (b) Al interlayer between layer #1 and #2.

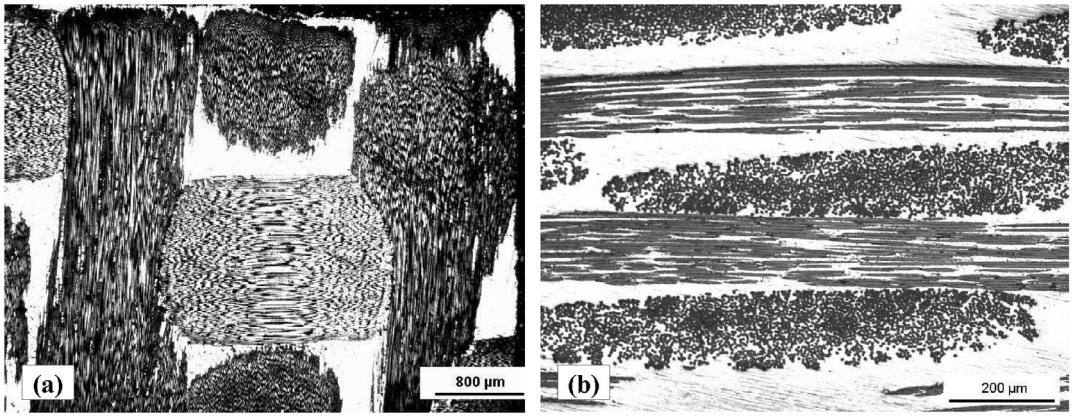

Fig 3 Optical micrographs of Mg/T300/w0/90° with stapled 0/90° (50%/50%) woven C-fiber fabric layers: (a) in plane, (b) cross-section.

2.2 Carbon reinforced Epoxy (CFRP)

The CFRP material is a T300 C-fiber reinforced epoxy CyCom 985GT-19-3 [8] (Epoxy/C-T300/55f). The investigated sample contains 8 UD layers of C-fiber bundles. The sample was embedded in an Araladit® epoxy cylinder in order to reduce the still significant beam hardening in the sample itself. From the optical micrograph in Fig.4 a fiber fraction of 55±3 vol.% was derived in reasonable agreement with the experimental density value of 1.55 g/cm³ obtained by a gravimetric method. The quantification of the local variations in fiber distribution by microscopy of cross sections of both CFRM and CFRP is destructive and very laborious, especially due to veins in between some fiber bundles.

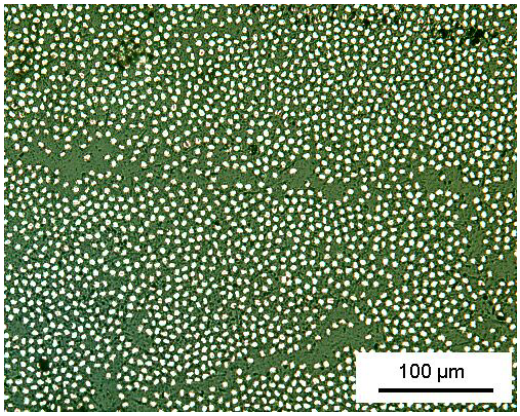

Fig. 4: Optical micrographs of cross sections of Epoxy/T300/55f showing the bundles with narrow matrix veins in between,

2.3 X-ray computed microtomography (µXCT)

Microtomography is based on the same physical principals and mathematical algorithms as the classical medical XCT-scanners as shown in Fig. 5a. A complete set of 2-dimensional X-ray radiographs of the object is recorded from different angular directions. For practical reasons, image detector and source are held in a fixed position and the sample is rotated. Cross section images are created using a filtered back-projection algorithm with convolution and correction for fan beam [9]. The reconstructed cross sections from all layers contain full 3D information about the object's internal morphology without special sample preparation or treatment. The method is limited to light weight materials and small dimensions, because the sample must be sufficiently transparent for X-rays of the available energy.

Recording of the images was made using the SkyScan-1072 high-resolution desk-top microtomograph [10]. This instrument has a warranted resolution of about 8 µm and under favorable conditions a detail detectability down to 3 µm. The system contains a sealed air cooled X-ray microfocus source 20-80 kV and a 2D cooled CCD detector with 1024×1024

pixels/12bit and pixel-size of 12 µm. The scintillator is coupled with a 2:1 reduction fiber optics, such that the total field of view is 25 millimeters. Magnification of the sample is obtained by projection of a "shadow" radiograph onto the detector. According to the general rule for tomographic reconstruction, the object should always remain inside the field of view of the X-ray cone. Hence the final resolution (voxel size) depends on the maximum diameter of the object: the resolution of 8 µm is limited by the X-ray source for objects <10 mm, whereas for objects >12 mm the resolution of the order of 25 µm is limited by the detector.

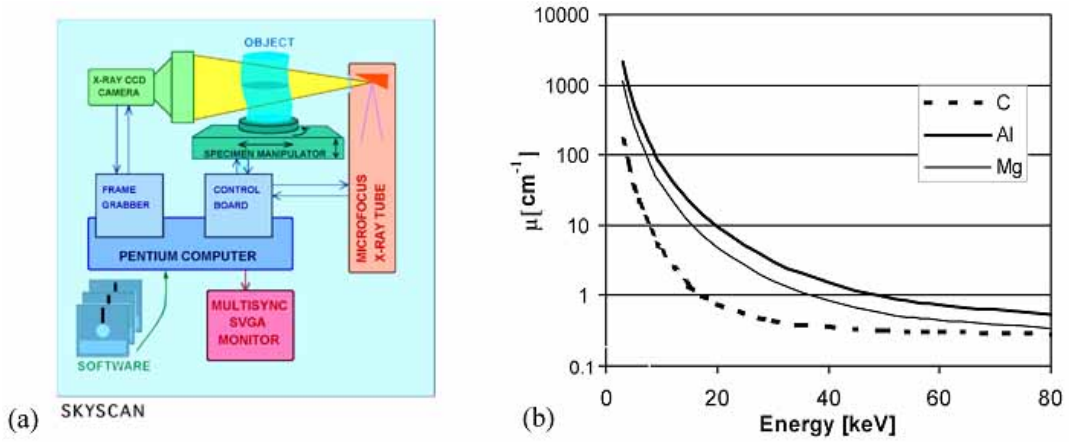

Fig. 5 (a) Diagram showing the micro-focus X-ray source, the sample manipulator and the high resolution array detector. (b) X-ray absorption coefficients of the constituents of the investigated CFRM calculated with XCOM [10].

The X-ray absorption coefficient for the constituents of the CFRM investigated depends on the X-rays' energy as shown in Fig. 5b 11]. The difference in absorption allows to distinguish between materials by discrimination of intensities transformed into gray values. Below 3 keV most of the X-rays are absorbed by the Be window of the X-ray tube. The spectral composition is shifted to the hard side of the spectrum, when the polychromatic beam penetrates the sample. The result is an apparent higher density at the rim of the sample, which causes the well known artifact of "beam hardening". This effect can be largely reduced by incorporation of an 0.8mm Al filter eliminating practically all X-rays below 15 keV, by using the standard SkyScan correction procedure based on actual transmission measurement on Al and by adjustments minimizing the cupping effect. The µXCT-recordings of the composites have been performed mostly at 50 kV and 100 µA current.

2.4 Three dimensional characterization of CFRM

The composite sample was scanned simultaneously with reference samples: commercially pure Al and Mg; a graphite electrode of 1.415 g/cm^3 density, the porosity of which cannot be resolved by µXCT. The manufacturer of the M40 fiber material gives a density of 1.81 g/cm^3, less than 2.26 g/cm^3 of dense graphite. After reconstruction of the µXCT images, all reference materials gave a Gaussian gray value distribution (see Fig. 7a). There remains some uncertainty regarding the linearity of the gray-scale. At a scale where air is set to 0, the mean gray values of the reference samples were determined at 205 for pure Al and at 29 for the electrode graphite, which was corrected to 37 for the higher density of C-fibers.

The example of a µXCT reconstruction given in Fig. 6 consists of 6 selected cross sections along an Al/M40/st0,±60° sample of 15×5×2 mm³, which has been cut 15° inclined to the fiber directions of layers #1 and #6. Matrix agglomerations between the differently oriented fiber layers (matrix interlayers) and between fiber bundles (matrix veins) can be seen as well as a crack running in the top layer #6, both parallel to the fibers. Some of the veins disappear

along the sample. The absence of an Al interlayer between the parallel layers #3 and #4 is confirmed (compare Fig.2). Layer #1 exhibits irregular fiber free matrix and a disordered fiber arrangement.

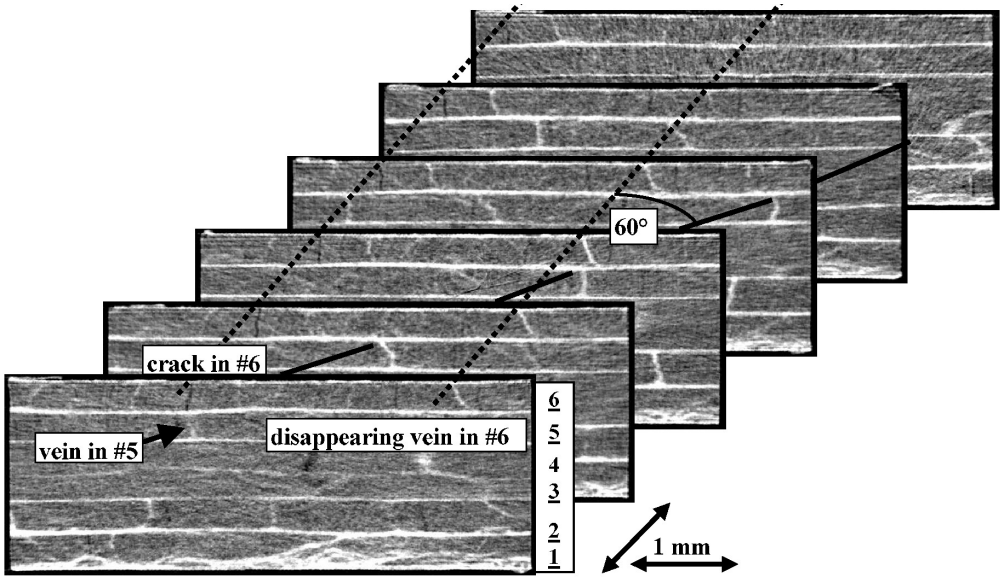

Fig. 6 µXCT sections through an Al/M40/st0,±60° sample (0° fiber direction 15° inclined to the specimen edge), showing 6 fiber layers with Al interlayers, various veins in the different layers, a crack parallel to the fibers in #6, irregular fiber distribution in #1.

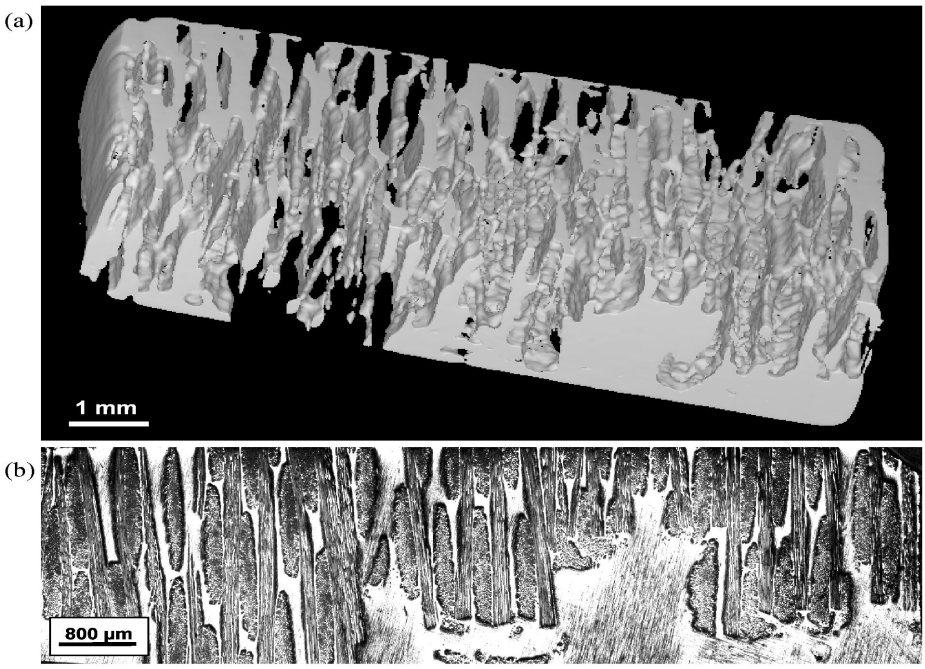

Fig. 7 Mg/T300/w0/90° sample region with missing fiber bundles: (a) iso-surface reconstruction from µXCT of the fiber free matrix region, (b) optical micrograph of a cross section.

One sample of Mg/T300/w0/90° contains fiber layers ending within the sample as shown in Fig. 7. The intensities of 3D µXCT recordings can be discriminated between the fiber free and reinforced matrix. The interface between the two regions was computed providing an iso-surface of the absorption contour of fiber-free Mg-matrix as depicted in Fig. 7a. In this way the shape of inhomogenities like fiber free regions and veins can be visualized in 3D.

3. RESULTS

3.1 Fiber packing

The quality of UD fiber reinforced composites can be quantified by comparison of the gray value histograms of CFRM samples with a benchmark curve, A perfectly infiltrated CFR-Al-sample of 2 g/cm³ mass density containing 75 vol.% unidirectional densely packed C-fibers provides a benchmark histogram,.an example of which is shown in Fig. 8a for 2 layers of the Al/M40/st0,±60° sample (see Fig. 6). The benchmark histogram is matched to the height of the gray value histogram of the test sample giving a corresponding histogram area B. Subtracting B from the area of the measured curve A yields the area beyond the benchmark distribution, which is related to the total area A of the gray value histogram yielding D = (A-B)/A, the relative deviation from a perfect CFRM. The difference P = 1-D indicates the degree of perfection in fiber packing and matrix density. The packing quality P, expressed in % of the benchmark distribution in Fig. 8a yields 100% for layer #3 and 78% for layer #1.

The whole Al/M40/st0,±60° sample can be validated by calculating P with respect to a perfect UD-CFRM. Fig. 8b gives the gray value distribution of the sample and the matched benchmark curve. The exceeding tail due to matrix interlayers and veins amounts to D=25% of that histogram. The packing quality of the whole sample is P=75%. An important quality criterion of planar samples is the symmetry of fiber arrangement in thickness with respect to the central plane. The µXCT data can be divided by the central plane and the two halves compared. Fig. 8b shows the histograms of the lower (layers #1-#3) and the upper half (layers #4-#6), with packing qualities of 67% and 83%, respectively. This considerable difference makes this CFRM sample behave like a bi-metal during temperature changes owing to the resulting local difference in thermal expansion [12].

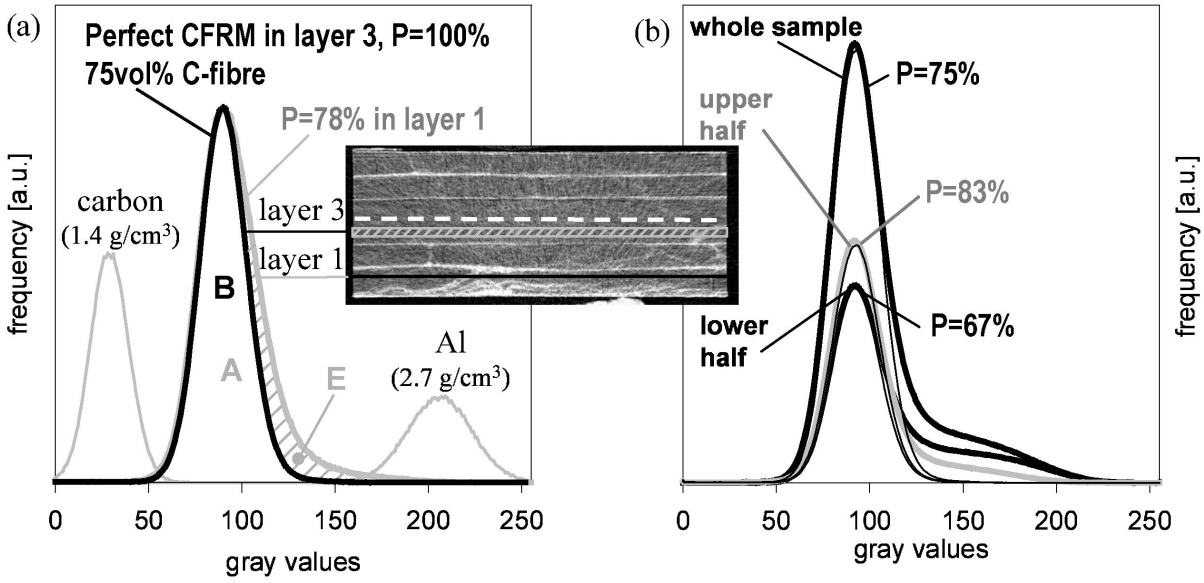

Fig 8 Gray value histograms of the Al/M40/st0,±60° sample, a cross section recorded by µXCT is inserted: (a) reference samples of constituents Al and C; B benchmark UD Al-CFRM with 75 vol.% fibers (equal to layer #3) compared with A of layer #1 yields P=78%. (b) Histograms of the whole sample (P=75%), layers #1-3 (lower half: P=67%) and layers #4-6 (upper half: P=83%);

3.2 Matrix layers in stapled fiber reinforcements

The matrix interlayers in CFRM reinforced by stapled textiles can be quantified by integrating the gray levels over planes parallel to the fibers as indicated in Fig. 9. The distance between the resulting density maxima gives the average thickness of each fiber layer D_S. There is no significant interlayer between the parllel layer #3 and #4. Layer #6 is the most densely packed of about 300 µm thickness. The deviation of layer #1 from perfect packing can be quantified locally, where the matrix accumulation increases gradually towards the sample's surface. The peak areas can be compared with a theoretical step function of fiber free aluminum (μ_{Al}) above the background level of the CFRM (μ_{MMC}) yielding a width for the same area of the measured curve above the CFRM background level, which represents the average thickness of the equivalent fiber free matrix interlayers D_{Al} as given in Fig.9. 16µm seems to be the minimum value achievable between different fiber orientations in this lay up system. More than 10% of the sample's thickness are occupied by the matrix interlayers.

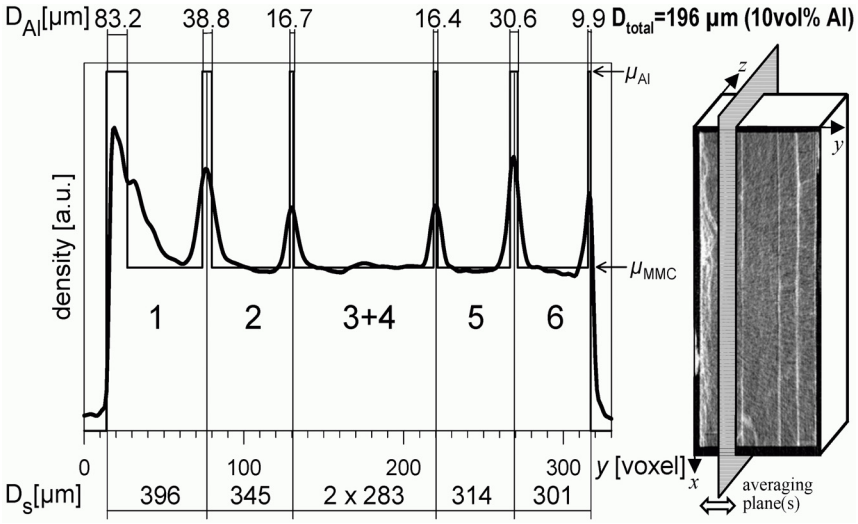

Fig. 9 Average density profile of the *x*/*z*-planes of µXCT of the Al/M40/st0,±60° sample as indicated in the insert (see Fig. 6): peaks at the Al interlayers of equal areas with the rectangles $(\mu_{Al}\text{-}\mu_{MMC})\cdot D_{Al}^{(i)}$, providing the indicated thickness values. The distances between the peaks yield the average thickness of the fiber layers $D_s^{(i)}$.

3.3 Distribution of woven fiber reinforcement

CFRM reinforced by woven textile fabrics contain fiber free matrix adjacent to each bundle cross over (see Fig.3). Fig. 10a/b illustrates in plane and cross sectional µXCT gray value distribution of a Mg/T300/w0/90° sample, where the bright areas of matrix accumulations can be observed.

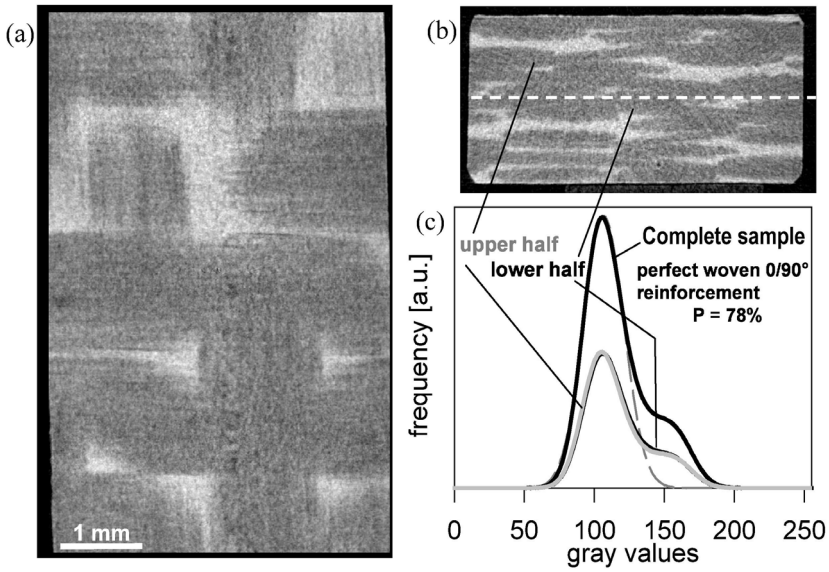

Fig. 10 Cross-sections (µXCT at 50 kV) of a perfect Mg/T300/w0/90° sample: (a) parallel to the woven fabric, (b) transverse: dark fiber bundles with bright matrix in between. (c) Histograms of gray values of the whole sample and of the two halves, all of them yielding P=78% in relation to the inserted benchmark histogram (dashed line) of a densely packed UD CFRM.

The fiber arrangement in this sample looks very dense and regular. Fig. 10c shows that the histogram for woven reinforcements yields a packing quality P = 78% with respect to densely packed UD-CFRM (Mg/M40/UD with v_f =70%), which corresponds to the determined average volume fraction of 0.78×70 vol.% = 55 vol.% fibers. Therefore the corresponding histogram of gray values can be taken as benchmark for Mg-samples with reinforcements of woven 0/90° high strength C-fibers. The symmetry check with respect to the central plane gives identical histograms for both halves of the sample.

The gray value histogram of an irregular section of a Mg/T300/w0/90° sample depicted in Fig. 7 yields a packing quality of about 40% with respect to UD-CFRM due to the fiber free matrix regions. The comparison with the benchmark histogram of the regular CFRM described in Fig. 10 results in a reinforcement quality of about 50% with respect to regular CFRM with 0/90° weave reinforcements.

3.4 Carbon reinforced epoxy sample

The µXCT recordings gave clear indication of the overall pattern of individual C-fiber bundles. The impregnated C-fiber bundles should show up with higher density due to the contribution of the stronger X-ray absorption of the carbon fibers compared with the fiber-free matrix in between as shown in the optical micrograph in Fig.11a. However, the recordings show the opposite: The central part of the bundles appears to be less dense than the borders. The optical image shows sharp and thin linings of matrix between the fiber bundles (see Fig.4), while much broader, dark markings are seen in the µXCT reconstructions (Fig 11b). Small, bright dotted lines are visible in the µXCT images within the high density regions, which are originated from interbundle distances as seen in optical images.

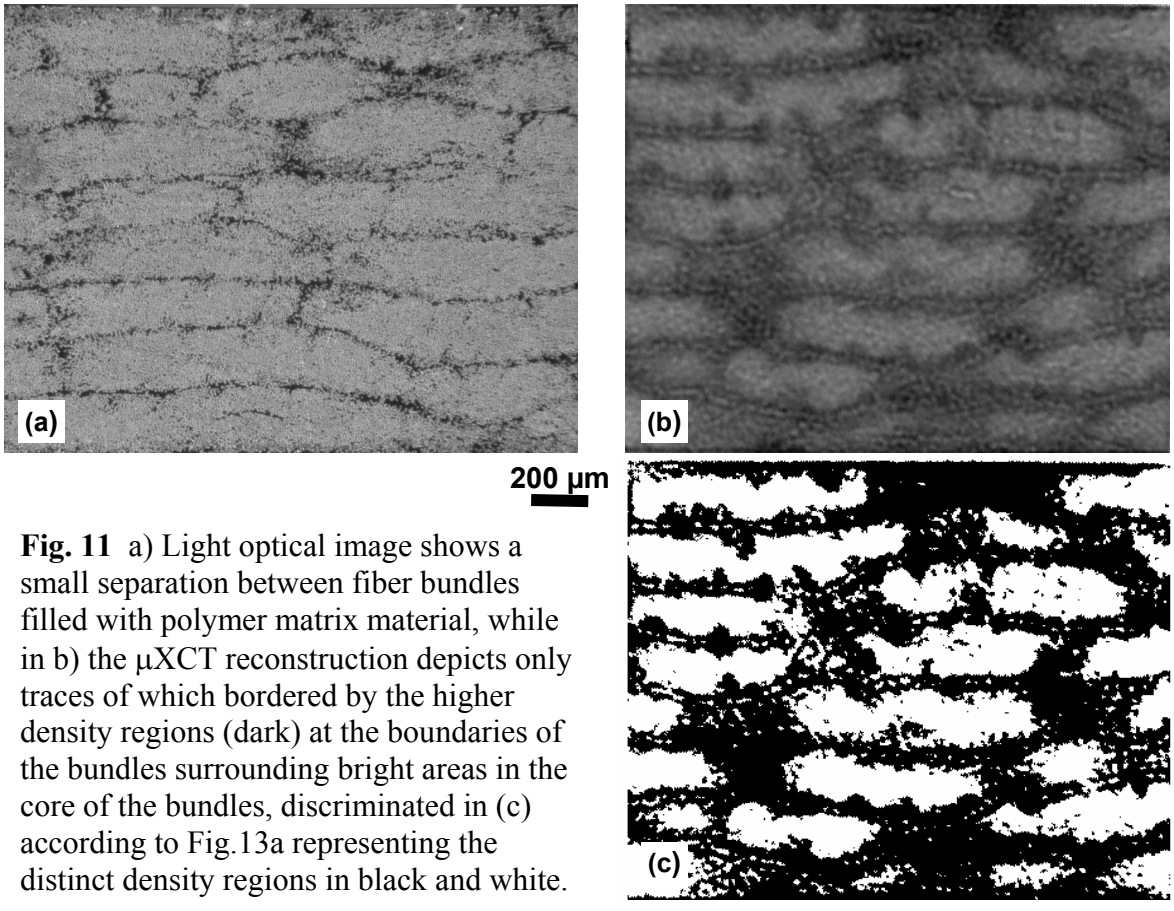

Fig. 11 a) Light optical image shows a small separation between fiber bundles filled with polymer matrix material, while in b) the µXCT reconstruction depicts only traces of which bordered by the higher density regions (dark) at the boundaries of the bundles surrounding bright areas in the core of the bundles, discriminated in (c) according to Fig.13a representing the distinct density regions in black and white.

The CFRP sample was cooled to embrittle the matrix and broken parallel to the fibers and the fracture surface was examined by scanning electron microscopy (SEM) looking for partial infiltration and porosity in the centres of the fiber bundles. Fig.12 shows that polymer matrix indeed penetrated the whole cross section of fiber bundles, but there are some voids in the range of some μm between individual fibers. The size of these voids is below the resolution of the μXCT instrument, but can explain a reduced average X-ray absorption in the central regions of the bundles. Any surface preparation would smear out such pores, so it seems that their statistical presence in CFRP can only be detected non-destructively by μXCT.

Fig 13a represents the distribution of the gray-values for all voxels in the CFRP sample, which look like a double peak. The enclosed histograms are obtained from selected areas in the central region of the fiber bundles and at their dense borders yielding average gray-values of 105 and 75, respectively. About 60% of the volume is occupied by dense fiber reinforced epoxy. Some 10% of the voxels belong to the region of gradual transition between the two defined density zones. The gray-values of the less dense regions of the CFRP contain as well the small contribution of the matrix in between the bundles, which cannot be separated by applying a threshold level discrimination. From Figure 13a we conclude that the main regions can reliably be separated using a simple threshold at gray-value 93, which is different to the average gray-value of the CFRP-sample being 87.The separation of the two defined density regions is shown in Fig. 11c, where they are digitised in white and black. In that picture the traces of the matrix material between the fiber bundles can be seen as well..

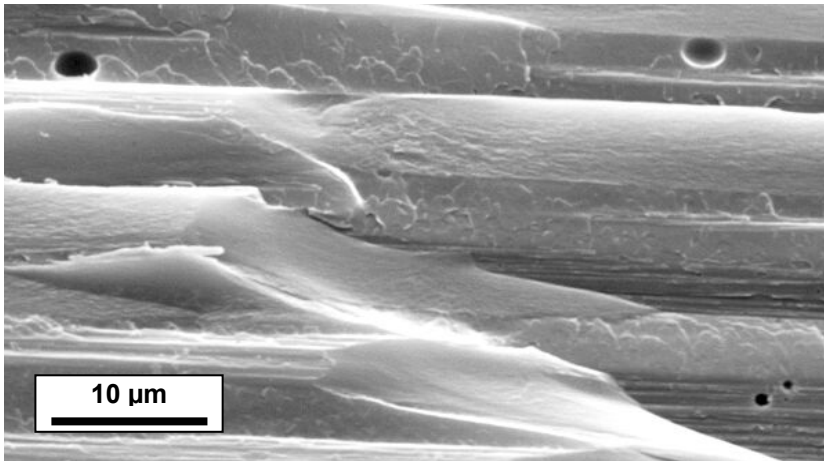

Fig. 12 Longitudinal fracture surface of a frozen CFRP sample revealing pores in the epoxy matrix between the fibers in the central region of the bundles.

The gravimetric values of the density for the embedding epoxy (Araldite of 1,2 g/cm³) and the CFRP material (1,55 g/cm³), together with the corresponding gray-values, being 205 and 87, respectively, are chosen as points of reference in a gray-value vs. mass density diagram as shown in Fig.13b. Approximating a linear function between mass density and XCT gray-values for the involved materials allows to inter- and extrapolate for the mass density values associated to the gray-values of the low and high density regions of the CFRP. The difference of 30 gray value units corresponds to ca. 0,09 g/cm³ change in mass density, which represents a span of about 6 % with respect to the average mass density of the CFRP. If a scatter of ± 3 vol.% in fiber volume fraction is taken into account (corresponds to a span of 2 mass % of the CFRP), a density difference of 4 % between the low and high density regions of the CFRP has

to be attributed to the matrix, the density of itself should therefore differ by about 8 %. Some contribution can be assigned to the identified porosity (Fig.12), which looks less than 8 vol.%.

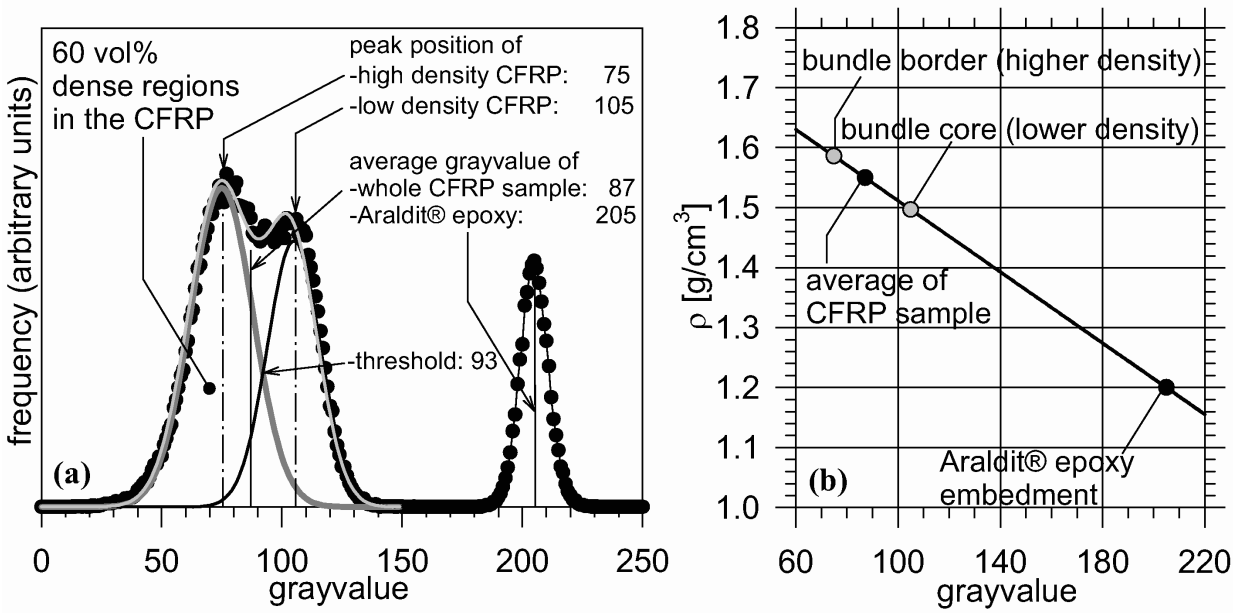

Fig. 13 a) Gray-values for the CFRP sample split up into the histograms of the two distinct fiber reinforced regions separated by the threshold 93: high density bundle borders and low density bundle centres with their mean gray-values and the histogram of the embed-ding Araldite®. b) Correlation of gray-values with density for the chosen beam hardening correction (reference points are the embedding Araldite® epoxy of 1,2 g/cm³ and CFRP-sample with 1,55 g/cm³) for inter- and extrapolation of unknown density regions.

4. CONCLUSIONS

X-ray computed tomography allows visualizing non-destructively the course of individual C-fiber bundles in light materials, which occupy cross sections bigger than 0.1 mm². Although µXCT was applied for samples of a few millimeters yielding a spatial resolution of ca.10µm, individual fibers cannot be resolved, but fiber bundles will be resolvable in samples up to diameters of 100 mm. The absorption contrast between C-fibers and Al, and even epoxy is high enough to distinguish unreinforced and reinforced matrix. The contrast between C-fibers and Mg is surprisingly high at low acceleration voltages owing to the photo-electric absorption difference. Density differences less than 0,05 g/cm³ can be resolved locally for volumes comprising about 10 slices of 5x5 voxels (ca.10^4 µm³). Defects like pores and cracks can be localised when bigger than 3x3x3 voxels (i.e. 1000µm³).

Fiber free regions can be discriminated and their contours can be depicted by iso-surfaces. In analogy regions of poor infiltration by the matrix can be identified as well and imaged as iso-surface. Fiber or matrix free regions can be quantified by the occupying volume fraction of the sample. The average thickness of interlayers in between fiber lay-ups can be calculated as well as maxima or minima can be localized in XCT recordings. The iso-surface technique can be applied to present the interface in selectively reinforced components. Materialographic pictures give only a local impression of the non-uniformity, whereas XCT provides quantitative 3D information.

The quality of fiber and matrix distribution within a composite can be quantified by gray value histograms, which represent different volume fractions of reinforcement up to fiber free matrix and matrix inhomogeneities up to uninfiltrated regions. Densely packed unidirectional reinforced homogeneous matrix provides histograms which can serve as a benchmark, when the fiber distribution is verified by materialography and the fiber volume fraction calibrated. The deviation of histograms from benchmark curves provides a quantitative measure of the correspondence to a perfect composite. Such benchmark histograms can be established for different fiber arrangements to serve as a quality criterion. The analysis of gray value histograms can be made for the whole sample as well as for segments of a sample to verify uniformity of both the reinforcement and the matrix.

Especially in the stage of development of a fiber reinforced component µXCT can serve as a tool for non-destructive determination of fiber arrangements and matrix imperfections before testing. In the course of production the specification of benchmark histograms can provide quantitative quality criteria, which in an automated process could be applied for online control.

ACKNOWLEDGEMENTS

The authors thank ARC-Leichtmetall-Kompentenzzentrum Ranshofen/Austria and the Institut für Leichtbau und Kunststofftechnik at the Technical University of Dresden/Germany for the provision of CFRM samples and the company FACC, Austriafor the CFRP sample

References

1 **Kelly A, Zweben C.**, ed. of Comprehensive Composite Materials, Elsevier, Oxford 2000
2 **Clyne TW**, ed. of Metal Matrix Composites, Vol. 3 of reference 1
3 **Degischer H.P**. Rammerstorfer FG, Beffort O, in Magnesium Alloys and their Applications, ed. K.U.Kainer, Wiley-VCH, Weinheim 2000, p. 207-214.
4 **Baruchel J, Buffiere JY, Maire E, Merle P, Peix** G, ed. of X-Ray Tomography in Material Science, Hermes, Paris 2000
5 **Capel H, Harris SJ, Schulz P, Kaufmann H**, Mat.Sci.&Techn. 2000; 16, p. 765-768
6 **Schreiber K, Hufenbach W, Langkamp A, Wagner L, Kottar A, Schulz P**; in Verbund-werkstoffen u. Werkstoffverbunde, ed. Wielage B, Wiley VCH, Weinheim 2001, p. 127-133.
7 **Mohammed A, Knoblich H, Kottar A, Degischer HP, Cornelis E, Schulz P, Langkamp A**: Continuous C-fiber alignment in Al and Mg matrices, in Fortschritte in d.Metallographie, Vol.34, ed. Kneissl A, Jeglitsch F, Werkstoffinformation GmbH, Frankfurt 2003, p. 475-482.
8 Boeing Material Specification 8-212, revised 28 july 1999.
9 **Herman G,** Image Reconstruction from Projections, Academic Press, London,1980.
10 **Sasov A,Van Dyck D**, J.of Microscopy 1998, 191, pt.2, p. 151-158.
11 http://physics.nist.gov/PhysRefData/
12 **Degischer HP, Mohammed A, Schulz P, Langkamp A**; Thermal expansion of C-fiber reinforced Mg and Al, submitted to Composites